ORIGINAL ARTICLE

JCSM Rapid Communications 2021; **4**: 207–221
Published online 15 June 2021 in Wiley Online Library (wileyonlinelibrary.com) **DOI:** 10.1002/rco2.44

Altered H19/miR-675 expression in skeletal muscle is associated with low muscle mass in community-dwelling older adults

Elie Antoun[1,12†], Eugenia Migliavacca[2†], Emma S Garratt[1], Sheila J Barton[3], Phil Titcombe[3], Leo D Westbury[3], Alica Baczynska[4], Richards Dodds[5,6], Helen C Roberts[4,7], Avan A Sayer[5,6], Sarah Shaw[3], H.E. Syddall[3], Allan Sheppard[8], Craig McFarlane[9], Neerja Karnani[10], Terrence Forrester[11], Cyrus Cooper[3,7], Jerome N Feige[2], Harnish P Patel[3,4,7‡], Keith M Godfrey[1,3,7‡], Karen A Lillycrop[1,7,12*‡] & the EpiGen Global Research Consortium

[1]*Human Development and Health Academic Unit, Faculty of Medicine, University of Southampton, Southampton, UK;* [2]*Nestle Research, EPFL Innovation Park, Lausanne, Switzerland;* [3]*MRC Lifecourse Epidemiology Unit, University of Southampton, Southampton, UK;* [4]*Academic Geriatric Medicine, Faculty of Medicine, University of Southampton, Southampton, UK;* [5]*Ageing Geriatrics & Epidemiology, Institute of Neuroscience, Newcastle, UK;* [6]*NIHR Newcastle Biomedical Research Centre, Newcastle University and Newcastle upon Tyne Hospitals NHS Foundation Trust, Newcastle upon Tyne, UK;* [7]*NIHR Southampton Biomedical Research Centre, University of Southampton and University Hospital Southampton NHS Foundation Trust, Southampton, UK;* [8]*Liggins Institute, University of Auckland, Auckland, New Zealand;* [9]*James Cook University, Townsville, Queensland, Australia;* [10]*Singapore Institute for Clinical Sciences, Singapore;* [11]*University of West Indies, Kingston, Jamaica;* [12]*Biological Sciences, University of Southampton, Southampton, UK*

Abstract

Background Despite increasing knowledge of the pathogenesis of muscle ageing, the molecular mechanisms are poorly understood. Based on an expression analysis of muscle biopsies from older Caucasian men, we undertook an in-depth analysis of the expression of the long non-coding RNA, *H19*, to identify molecular mechanisms that may contribute to the loss of muscle mass with age.

Methods We carried out transcriptome analysis of *vastus lateralis* muscle biopsies from 40 healthy Caucasian men aged 68–76 years from the Hertfordshire Sarcopenia Study (HSS) with respect to appendicular lean mass adjusted for height (ALMi). Validation and replication was carried out using qRT-PCR in 130 independent male and female participants aged 73–83 years recruited into an extension of the HSS (HSSe). DNA methylation was assessed using pyrosequencing.

Results Lower ALMi was associated with higher muscle *H19* expression ($r^2 = 0.177$, $P < 0.001$). The microRNAs, *miR-675-5p/3p* encoded by exon 1 of *H19*, were positively correlated with *H19* expression (Pearson $r = 0.192$ and 0.182, respectively, $P < 0.03$), and *miR-675-5p* expression negatively associated with ALMi ($r^2 = 0.629$, $P = 0.005$). The methylation of CpGs within the H19 imprinting control region (ICR) were negatively correlated with *H19* expression (Pearson $r = -0.211$ to -0.245, $P \leq 0.05$). Moreover, RNA and protein levels of *SMAD1* and *5*, targets of *miR-675-3p*, were negatively associated with *miR-675-3p* ($r^2 = 0.792$ and 0.760, respectively) and *miR-675-5p* ($r^2 = 0.584$ and 0.723, respectively) expression, and *SMAD1* and *5* RNA levels positively associated with greater type II fibre size ($r^2 = 0.184$ and 0.246, respectively, $P < 0.05$).

Conclusions Increased expression profiles of *H19/miR-675-5p/3p* and lower expression of the anabolic *SMAD1/5* effectors of bone morphogenetic protein (BMP) signalling are associated with low muscle mass in older individuals.

Keywords Muscle mass; Long non-coding RNA; SMAD

Received: 11 January 2021; Revised: 27 April 2021; Accepted: 12 May 2021
**Correspondence to: Karen Lillycrop, Human Development and Health Academic Unit, Faculty of Medicine, University of Southampton, Southampton, SO16 6YD, UK. Phone: +442380593332, Fax: +442380595545, Email: kal@soton.ac.uk*
†These authors are joint first authors.
‡These authors are joint senior authors.

Introduction

A decline in muscle mass and strength is a fundamental consequence of ageing. Adequate skeletal muscle is essential for all aspects of physical function, as well as for metabolism and thermoregulation; consequently, the progressive loss of muscle mass and strength with advancing age is associated with a number of adverse physical and metabolic changes.[1,2]

The maintenance of muscle mass is controlled by multiple interconnected signalling pathways, which regulate anabolic and catabolic signals in the muscle and the balance between muscle atrophy and hypertrophy.[3] During ageing, this balance is disrupted, with a decline in the production of anabolic hormones and increased anabolic resistance,[4] impaired protein synthesis,[5] denervation,[6] loss of regenerative muscle satellite cell activity,[7,8] and reduced mitochondrial function, which results in decreased muscle mass and function.[9,10] The expression and/or activity of many of the genes that regulate these processes, or co-ordinate the integration of the signalling pathways such as insulin-like growth factor 1,[11] the androgen receptor,[12] 5′ adenosine monophosphate-activated protein kinase,[13] myostatin,[14] Notch,[15] WNT,[16] Sirtuin 1,[17] and Id myogenic repressors,[18] have also been reported to be altered in ageing muscle. Consistent with these findings, transcriptomic studies either using expression arrays or RNAseq on muscle biopsies from young versus old individuals have shown increased expression of pathways regulating cell growth, complement activation, ribosomal and extracellular matrix genes, as well as RNA binding/processing proteins, and components of the ubiquitin-proteasome proteolytic pathway in older muscle, while genes enriched in pathways associated with chloride transport and mitochondrial oxidative phosphorylation were down-regulated.[19–21]

However, there is significant variability between individuals in the rate of loss of muscle mass in old age. Some of the variability can be explained by fixed genetic factors,[22,23] but much of the remaining variation is unexplained. To date, most of the studies that have identified genes associated with muscle ageing have compared changes in muscle tissue from young versus old individuals, and the contribution that these genes make to the variability observed between older individuals in terms of loss of muscle strength and mass is unknown. To address this, we recently compared muscle transcriptomic profiles from individuals with sarcopenia compared with healthy aged matched controls from the Singapore Sarcopenia Study and found that the major transcriptional pathway associated with sarcopenia was mitochondrial dysfunction, with similar pathways altered with respect to sarcopenia in the Hertfordshire Sarcopenia Study (HSS) and the Jamaica Sarcopenia Study (JSS).[21] To identify the changes in transcription associated with the loss of muscle mass, one of the definitional components of sarcopenia, here, we report the transcriptomic analysis of skeletal muscle biopsies from older individuals from the HSS with respect to appendicular lean mass index (ALMi), together with an in-depth analysis of the expression of the long non-coding RNA, *H19*, the top transcript positively associated with ALMi to identify molecular mechanisms that may contribute to the loss of muscle mass with age.

Methods

Study participants

All participants were recruited from the UK Hertfordshire Cohort Study (HCS).[24] The HSS, a sub-study of the HCS, was designed to investigate life course influences on muscle morphology, mass, and strength in community-dwelling older people. The first phase of the study has previously been described in detail.[25] The second, extension phase of the study (HSSe) recruited a total of 168 men and women. The skeletal muscle characterization carried out in this study included total lean mass and body composition ascertained by dual-energy X-ray absorptiometry (DXA) scanning, handgrip strength determined by using a Jamar hydraulic dynamometer (Promedics, UK), and physical capability measured by gait speed timed over 3 m.[26] Percutaneous muscle biopsies of the *vastus lateralis* were conducted after an overnight fast under local anaesthetic using a Weil-Blakesley conchotome.[27] A portion of muscle tissue was used for cell culture while another portion was snap frozen in cooled isopentane and stored at −80°C until further analysis.

Out of the 105 male participants recruited in the HSS, 40 were selected for RNAseq analysis; these were the only samples that had sufficient RNA for RNAseq analysis. Fifty-seven HSS samples were analysed by qRT-PCR; this included 37 samples analysed by RNAseq (six had insufficient RNA remaining after the RNAseq analysis) and 20 additional samples for which there was sufficient RNA for qRT-PCR analysis. This approach was taken to increase power for the qRT-PCR analysis. Following QC of the qRT-PCR data, three of the 37 samples with RNAseq data and two of the 20 additional samples failed QC (melt curves showing primer dimers) and were excluded from the analysis, leaving a total of 52 samples with qRT-PCR data (34 with RNAseq data and 18 additional HSS samples).

To replicate the findings in an independent cohort and to determine whether the association was observed in both men and women, qRT-PCR was also carried out on 130 male

and female participants from the HSSe; these were the only participants with sufficient RNA. Myoblast cultures from a total of nine biopsies were used for transfection analysis to determine the causal role for H19 in regulating human skeletal muscle mass. A schematic for all the samples used in the different analyses can be found in Supporting Information, *Figure S1*. The study received ethical approval from the Hertfordshire Research Ethics Committee (Number 07/Q0204/68) and conducted in accordance with the 1964 Declaration of Helsinki and its later amendments.

RNA extraction

RNA from muscle tissue was extracted using the mirVana miRNA Isolation Kit (ThermoFisher Scientific). Frozen muscle samples were placed into 600 μL Lysis/Binding buffer and homogenized using a Dispomix Homogenizer (Miltenyi Biotech) until all visible clumps were dispersed. The isolation procedure was then performed according to the manufacturer's instructions using the total RNA isolation protocol. RNA was eluted in a volume of nuclease free water necessary to give a concentration $>$25 ng/μL (40–100 μL). Quantity and quality of total RNA was measured by Nanodrop (ThermoFisher Scientific), Qubit 2.0 Fluorometer (ThermoFisher Scientific), and Bioanalyzer (Agilent Technologies). All RNA had a RIN of $>$8.0. Total RNA was stored at $-$80°C.

RNAseq

RNAseq was carried out as previously described.[21] Briefly, 250 ng of total RNA was employed as starting material for library preparation. Sequencing libraries were prepared using the TruSeq Stranded Total RNA HT kit with the Ribo-Zero Gold module (Illumina), followed by 13 cycles of PCR amplification with the KAPA HiFi HotStart ReadyMix (Kapa BioSystems). Libraries were quantified with Picogreen (Life Technologies), and size pattern was controlled with the DNA High Sensitivity Reagent kit on a LabChip GX (Perkin Elmer). Libraries were then pooled at an equimolar ratio and clustered at a concentration of 7 pM on paired-end sequencing flow cells (Illumina). Sequencing was performed for 2 × 101 cycles on a HiSeq 2500 (Illumina) with v3 chemistry. The generated data were demultiplexed using Casava. Reads were aligned to the human genome (hs_GRCh38.p2) using TopHat,[28] and the number of reads mapped within genes was quantified by HTSeq[29] (Version HTSeq-0.6.1p1, mode union, strand reverse, quality alignment greater than 10). This procedure resulted in a sequencing depth of 51–110 million reads per sample, out of which 38–84 million were uniquely mapped. Data are publicly available from GEO under Accession Numbers GSE111006, GSE111010, and GSE111016 and integrated in the series GSE111017.

Bioinformatic analysis

Differentially expressed genes with respect to ALMi were determined using the DESeq2 package[30] (v1.18.1) in R (v3.2.1). Briefly, data were normalized using the relative log expression normalization method implemented in DESeq2. Independent filtering was carried out as default by removing genes with low expression. *P*-values were corrected for multiple testing using the Benjamini–Hochberg method with genes with a false discovery rate (FDR) $<$ 0.2 classed as differentially expressed.

Quantitative real-time PCR

Quantitative real-time PCR (qRT-PCR) was carried out using a LightCycler 480 Real-Time PCR System (Roche, UK); 500 ng total RNA was used as a template to prepare cDNA. RNA was DNase treated (Sigma, UK) and reverse transcribed to cDNA with the miScript II Reverse Transcription system (Qiagen). cDNA was amplified with commercial real-time qRT-PCR primers (Qiagen Quantitect, UK) using QuantiFast SYBR Green Mastermix (Qiagen) according to the manufacturer's recommendations. The reaction was performed in a total volume of 10 μL. Samples were measured in duplicate, and all technical replicates had a standard deviation (SD) $<$ 1. Results were analysed using the comparative CT ($2^{-\Delta\Delta CT}$) method. Housekeeping genes were identified by GeNorm analysis (Primer Design, UK). Ct values for mRNA analysis were normalized to two endogenously expressed housekeeping genes (PPIA and CYC1). Ct values for miRNA analysis were normalized to four endogenously expressed small RNAs (RNU6, SNORD61, SNORD68, and SNORD96A). For *H19* expression, cDNA was amplified using custom designed primers (Primer Design) using the Taqman Gene Expression Master Mix (ThermoFisher Scientific) according to the manufacturer's recommendations. List of primers used are shown in *Table S1*, and melt curves in *Figure S2*.

Quantitative DNA methylation analysis

Genomic DNA was extracted from frozen muscle tissue by classical proteinase K digestion and phenol:chloroform extraction; 500 ng DNA was bisulfite converted using the EZ DNA Methylation Gold Kit (Zymo Research, Ivrine, CA) per the manufacturer's protocol. PCR primers specific for bisulfite-converted DNA were designed using EpiDesigner (Agena). Each reverse primer contained a T7-promoter tag for *in vitro* transcription (5′-cagtaat acgactcactatagggagaaggct-3′), while the forward primer had a 10mer tag to balance melting temperatures (5′-aggaagagag-3′). The list of primers used are shown in *Table S1*. Quantitative DNA methylation analysis was carried

DOI: 10.1002/rco2.44

out using the Sequenom MassARRAY Compact System (Agena). Bisulfite-converted DNA was amplified (Qiagen HotStar Taq Polymerase), and Shrimp Alkaline Phosphatase treated (Agena). Heat inactivation and simultaneous *in vitro* transcription/uracil-cleavage reaction was subsequently carried out. Products were desalted and spotted on a 384-pad SpectroCHIP (Agena) using a MassARRAY nanodispender (Samsung). Spectra were acquired using a MassArray MALDI-TOF MS, and peak detection and quantitative CpG methylation carried out using the EpiTyper software v1.0 (Agena).

Myoblast cultures

Biopsies were collected into 30 mL PBS and processed within 1 h of biopsy and digested with 2 mg/mL Collagenase Type 1A in DMEM for 20 min at 37°C. The resulting suspension was spun at 2200 g for 10 min and resuspended in 12 mL PBS. Any remaining cell clumps were disassociated with a pipette prior to being filtered through a 100 μm cell strainer. This cell suspension was centrifuged and resuspended in prewarmed proliferation media [DMEM containing 20% FBS, 10% horse serum, 1% chick embryo extract (CEE), and 1% penicillin/streptomycin]. To remove any contaminating fibroblasts, the cell suspension was added to a non-matrigel coated 10 cm cell culture dish and incubated at 37°C for 3 h. The cell suspension was then transferred onto a new matrigel-coated plate (10% matrigel in DMEM) and incubated at 37°C for 2 days. Media were then changed daily. Cell populations were trypsinized when they were 80% confluent. In order to differentiate myoblast cultures into myotubes, myoblasts were plated and grown to confluence with subsequent substitution of proliferation media with differentiation media (DMEM containing 2% horse serum and 1% penicillin/streptomycin). Cells were shown to be of myogenic origin by staining with CD56.[31]

Transfection of siRNAs and mature microRNAs

Myotube cultures were transfected with siRNAs or miRNA mimics at Passage 3; 10 pmol siRNA against H19 (Ambion) and 10 pmol *miR-675-3p/5p* miRNA mimics (Ambion) were transfected using the Lipofectamine RNAiMAX Transfection Reagent (Life Technologies) following the manufacturer's protocol. Briefly, myoblasts were grown to confluence in proliferation media, cells were washed, and media changed to differentiation media (Day 0). Lipofectamine:siRNA/miRNA complexes were added to the cells at Day 1 for 72 h. After 72 h, media were changed for fresh differentiation media and cells allowed to differentiate for a further 2 days. At Day 5, myotubes were harvested and frozen at −80°C untilRNA/protein extraction. RNA from transfected myoblasts/myotubes was extracted using Tri reagent (Sigma) following the manufacturer's instructions. Quantity and quality of total RNA was measured by Nanodrop (ThermoFisher Scientific). Total RNA was stored at −80°C until further use.

Western blotting

Muscle tissue was homogenized using a handheld bio-vortexor homogenizer. Protein lysates from muscle tissue were prepared in extraction buffer containing 50 mM Tris (pH 7.5), 150 mM NaCl, 50 mM NaF, 1 mM EDTA, 0.5% Triton X-100 with 1 mM PMSF, and 0.25% leupeptin. Total protein lysate concentrations were determined using a Pierce BCA Colorimetric Protein Quantitation Assay (Thermo Scientific, UK) and absorbance at 560 nm measured on the GloMax Plate Reader (Promega). Due to the limited amount of muscle tissue available, protein lysate from nine HSS muscle samples were analysed; these were the only samples with sufficient material remaining after RNA extraction. Twenty micrograms of protein lysate was added to an equal volume of loading buffer [125 mM Tris (pH 6.8), 200 mM DTT, 4% SDS, 20% glycerol, and 0.2% bromophenol blue]. Denatured protein lysate was resolved by 10% SDS PAGE. Protein transfer was performed in buffer containing 25 mM Tris, 192 mM glycine, 20% (v/v) methanol, and 0.1% (w/v) SDS. The membrane was blocked with 5% (w/v) dried skimmed milk powder (Marvel, UK) in 1× TBS containing 0.05% (v/v) Tween-20. Membrane sections were incubated overnight at 4°C with primary antibody diluted in blocking buffer followed by incubation with horseradish peroxidase-conjugated secondary antibody. Primary antibodies used were anti-SMAD5 (1:1000, 9517S, CST), anti-SMAD1 (1:1000, ab33902, Abcam), and anti-beta actin (1:1000, ab8224, Abcam). For SMAD1, two bands were consistently visible with the anti-SMAD1 antibody, the larger molecular weight band however was efficiently competed out using a SMAD1 peptide (ab66722, Abcam, *Figure S3*), and only the larger molecular weight band was quantified. Secondary antibodies used were goat anti-rabbit IgG H&L (HRP) (1:1000, ab6721, Abcam) and rabbit anti-mouse IgG H&L (HRP) (1:1000, ab6728, Abcam). Protein bands were detected using SuperSignal West Pico Plus Chemiluminescent Substrate (Thermo Scientific). Blots were imaged using a ChemicDoc XRS System (Biorad), with five images taken with exposures of 30, 60, 90, 120, and 150 s. The image with an exposure of 90 s was used for quantification, as this was within the linear range for quantification. Protein band intensities were analysed using ImageJ software from raw data images. Briefly, densitometry of the background blot was subtracted from the band of interest, followed by normalization to the loading control for each sample. β-Actin was used as a loading control protein to allow normalization of protein loading. Full images of the western blots are shown in *Figure S4*.

Immunohistochemistry

Immunohistochemistry was carried out on the muscle biopsies of men from the HSS as previously described in Patel *et al*.[32] Briefly, muscle tissue was fixed overnight at −20°C before being embedded in glycol methacrylate resin. Serial cross-sections at 7 μm were cut and stained for type II fast-twitch myofibres using the monoclonal anti-myosin fast antibody at a dilution of 1:6000 (clone MY-32; Sigma-Aldrich, Dorset, UK). Stained sections were examined under a photomicroscope (Zeiss Axioskop II, Carl Zeiss Ltd, Welwyn Garden City, UK) coupled to KS 400 image analysis software (Image Associates, Bicester, UK). Sections were viewed at ×5 magnification and digitized to obtain tissue area, myofibre number (type I, slow fibre vs. type II, fast fibre), and myofibre cross-sectional areas (μm^2). Slow and fast fibre proportions were expressed as a percentage of total fibres. Muscle morphology parameters were analysed in all samples by a blinded observer.[31]

Statistical analysis

Regression analysis was used to analyse the expression of genes with respect to the measures of muscle mass. The regression analyses were carried out with age as a covariate in the model for HSS participants, age and sex for the HSSe cohort, and age, sex, and batch in the combined HSS and HSSe data sets. All data were normally distributed, histograms were checked to determine the normality of the distribution of the residuals, and deviations in the QQ plot (standardized residuals vs. theoretical quantiles) were examined. All regression statistics reported are from multivariate regression models (*Tables S2* and *S3*). Correlation analysis was performed using Pearson correlation to compare the expression of the different genes. In transfection experiments to determine the effect of *H19* knockdown or ectopic expression of *miR-675-3p/5p*, a paired *t*-test was used.

Results

Participant characteristics

Summary of anthropometric and physical function of participants of HSS and HSSe is shown in *Table* 1. In HSS, all participants were male, the mean age (SD) was 72.63 years (2.47), height 1.74 m (0.07), weight 82.59 kg (13.06), body mass index (BMI) 27.33 kg/m^2 (3.51), total lean body mass 56.02 kg (6.66), appendicular lean mass 24.06 kg (3.23), total fat mass 22.32 kg (7.28), gait speed 1.11 m/s (0.19), and grip strength 37.56 kg (7.96). In HSSe, 29.3% (n = 38) of participants were male. The mean (SD) age was 78.45 years (2.55), height 1.64 m (0.08), weight 72.36 kg (11.64), BMI 27.05 kg/m^2 (3.88), total lean body mass 39.77 kg (6.98), appendicular lean mass 16.65 kg (3.49), total fat mass 29.00 kg (8.24), gait speed 0.96 m/s (0.20), and grip strength 25.17 kg (8.87).

Lower appendicular lean mass index is associated with changes in the muscle transcriptome

To investigate changes in the muscle transcriptome that may contribute to differences in muscle mass in older individuals, total RNAseq was carried out on 40 muscle biopsies from the vastus lateralis from male participants from the HSS and used to identify genes whose expression was associated with ALMi. The analysis of the RNAseq data showed that there were 23 transcripts associated with ALMi (FDR $<$ 0.25), of which four had an FDR $<$ 0.05 (*Figure* 1). There were *H19* (FDR = 0.019) and Ankyrin Repeat Domain 20 Family Member A1 (*ANKRD20A1*, FDR = 0.035), both negatively associated with ALMI, and SH3 domain binding kinase family member 2 (*SBK2*, FDR = 1.34E-06) and paired-like homeodomain 1 (*PITX1*, FDR = 1.19E-04), both positively associated with ALMi (*Table* 2).

Table 1 Cohort characteristics

	HSS (n = 57)		HSSe (n = 130)		HSSe male (n = 38)		HSSe female (n = 92)	
	Mean	SD	Mean	SD	Mean	SD	Mean	SD
Male (%)	100%		29.2%		NA		NA	
Age (years)	72.63	2.46	78.45	2.55	78.28	2.68	78.52	2.50
Height (m)	1.74	0.07	1.64	0.08	1.73	0.06	1.60	0.06
Weight (kg)	82.59	13.06	72.36	11.64	78.15	10.65	69.97	11.23
BMI (kg/m^2)	27.33	3.51	27.05	3.88	26.17	3.24	27.42	44.08
Total lean body mass (kg)	56.02	6.66	39.77	6.98	48.77	4.92	36.56	4.28
Appendicular lean mass (kg)	24.06	3.23	16.65	3.49	21.06	2.49	15.04	2.17
Total fat mass (kg)	22.32	7.28	29.00	8.24	25.08	7.94	30.39	7.93
Gait speed (m/s)	1.11	0.19	0.96	0.20	1.00	0.22	0.94	0.18
Grip strength (kg)	37.56	7.96	25.17	8.87	35.74	6.67	20.76	5.17

BMI, body mass index; HSS, Hertfordshire Sarcopenia Study; HSSe, Hertfordshire Sarcopenia Study extension; NA, not applicable; SD, standard deviation.

Figure 1 RNAseq differential expression with respect to appendicular lean mass index (ALMi) in muscle biopsies. (*A*) Volcano plot of the *P*-values versus log2 fold change. Genes with an FDR < 0.05 are shown in red, and those with an FDR between 0.05 and 0.25 shown in green. (*B*) Normalized count of H19 from the RNAseq plotted against ALMi showing a negative association.

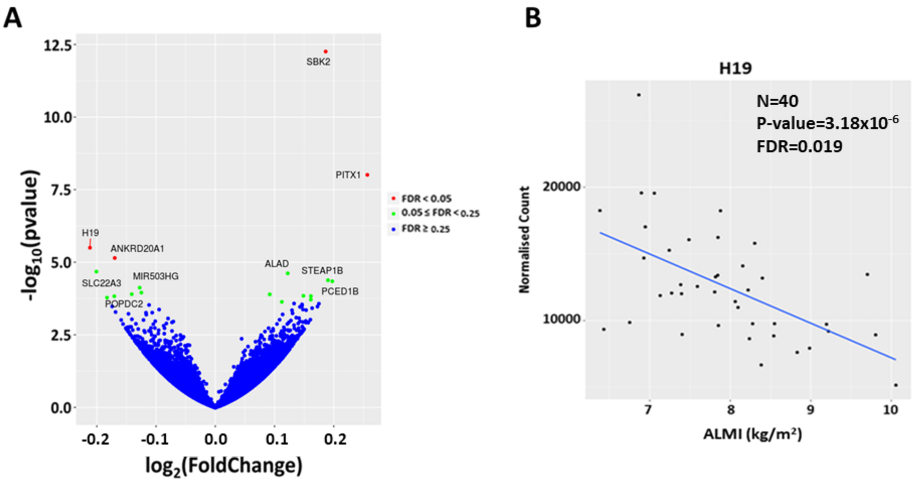

Higher H19 expression was associated with lower appendicular lean mass index

In the RNAseq analysis, the transcript most significantly down-regulated with respect to ALMi was *H19*, a long non-coding RNA which is expressed primarily in muscle tissue after birth, and which was previously reported by Lewis *et al*., to be inversely associated with low lean mass in chronic obstructive pulmonary disease (COPD) patients.[33] To validate the association between higher *H19* expression and lower ALMi, qRT-PCR was used. In 52 HSS samples (which included 34 samples with RNAseq data and 18 additional HSS samples for which there was enough RNA for qRT-PCR analysis), higher *H19* expression was associated with lower ALMi (r^2 = 0.081, *P* = 0.056, *Figure* 2A). When restricting the analysis to the samples for which there were both RNAseq and qRT-PCR data (*n* = 34), the association was weakened slightly (*P* = 0.128, *Figure S5*).

Table 2 List of differentially expressed genes with respect to appendicular lean mass index (false discovery rate < 0.25)

ENSEMBL gene ID	Estimate	*P*-value	FDR	Gene symbol
Up-regulated				
ENSG00000187550	0.19	5.53E-13	1.34E-08	SBK2
ENSG00000069011	0.26	9.81E-09	1.19E-04	PITX1
ENSG00000148218	0.12	2.42E-05	0.073	ALAD
ENSG00000105889	0.19	4.18E-05	0.096	STEAP1B
ENSG00000179715	0.2	4.54E-05	0.096	PCED1B
ENSG00000157330	0.09	1.28E-04	0.180	C1orf158
ENSG00000172461	0.15	1.44E-04	0.180	FUT9
ENSG00000117602	0.16	1.94E-04	0.214	RCAN3
ENSG00000211890	0.11	2.32E-04	0.244	IGHA2
Down-regulated				
ENSG00000130600	−0.21	3.18E-06	0.019	H19
ENSG00000260691	−0.17	7.17E-06	0.035	ANKRD20A1
ENSG00000146477	−0.2	2.11E-05	0.073	SLC22A3
ENSG00000223749	−0.13	7.52E-05	0.130	MIR503HG
ENSG00000121577	−0.14	1.26E-04	0.180	POPDC2
ENSG00000134107	−0.17	1.49E-04	0.180	BHLHE40
ENSG00000182841	−0.12	1.12E-04	0.180	RRP7BP
ENSG00000111664	−0.18	1.66E-04	0.191	GNB3

FDR, Benjamini–Hochberg adjusted false discovery rate.

To replicate the findings in an independent set of individuals and to examine whether the association was observed in both men and women, *H19* expression in relation to ALMi was also analysed in 130 male and female individuals from the HSSe cohort. Higher *H19* expression was associated with lower ALMi in the HSSe (r^2 = 0.465, *P* < 0.001, *Figure* 2B) study group. When stratifying by sex, we found that the association between *H19* and ALMi was significant in both men and women (men *P* = 0.016, women *P* = 0.001), albeit weaker in the men due to a smaller sample size. Moreover, when data from both HSSe and HSS were combined, a significant inverse association between *H19* expression and ALMi was observed (r^2 = 0.650, *P* < 0.001, *Figure* 2C and *Table S2*). There was also an inverse association between *H19* expression and gait speed (*P* = 0.040, *Figure* 2D) but no association with grip strength (*P* = 0.615) in the combined HSS and HSSe study group.

H19 imprinting control region methylation

As *H19* is a maternally imprinted gene, in which DNA methylation plays an important regulatory role, we assessed levels of DNA methylation at CpG sites within the CTCF regulatory binding sites in the imprinting control region (ICR) of *H19* in the HSSe samples. The methylation of CpGs within CTCF binding site 6 (CTCF6—CpG-2098: *r* = −0.231, *P* = 0.043; CpGs-2103/-2105: *r* = −0.245, *P* = 0.038) and CTCF binding site 3 (CTCF3) as well as three neighbouring CpGs

(CpGs-4344/-4347/-4349/-4351: $r = -0.211$, $P = 0.049$; CpGs-4288/-4290/-4294: $r = -0.218$, $P = 0.042$) showed a negative correlation with *H19* expression (*Table* 3). Methylation of CpG-2098 and CpGs-2103/-2105 within the CTCF binding site 6 were also positively associated with ALMi ($r^2 = 0.341$, $P = 0.036$ and $r^2 = 0.373$, $P = 0.037$, respectively) (*Table* 4).

Figure 2 Validation and replication of the expression of *H19* in HSS and HSSe muscle tissue determined by qRT-PCR. (*A*) Association between *H19* expression and ALMi in HSS study group. (*B*) Association between *H19* expression and ALMi in HSSe. (*C*) Association between *H19* expression and ALMi in combined HSS and HSSe data sets. (*D*) Association between *H19* expression and gait speed in combined HSS and HSSe data sets. Green points are HSSe samples while black points are HSS samples. Statistics are from a multivariate regression model with adjustment for age in HSS (*A*), age and sex in HSSe (*B*), and age, sex, and batch in the combined HSS and HSSe data sets (*C* and *D*). Regression coefficients for all models can be found in *Table S2*.

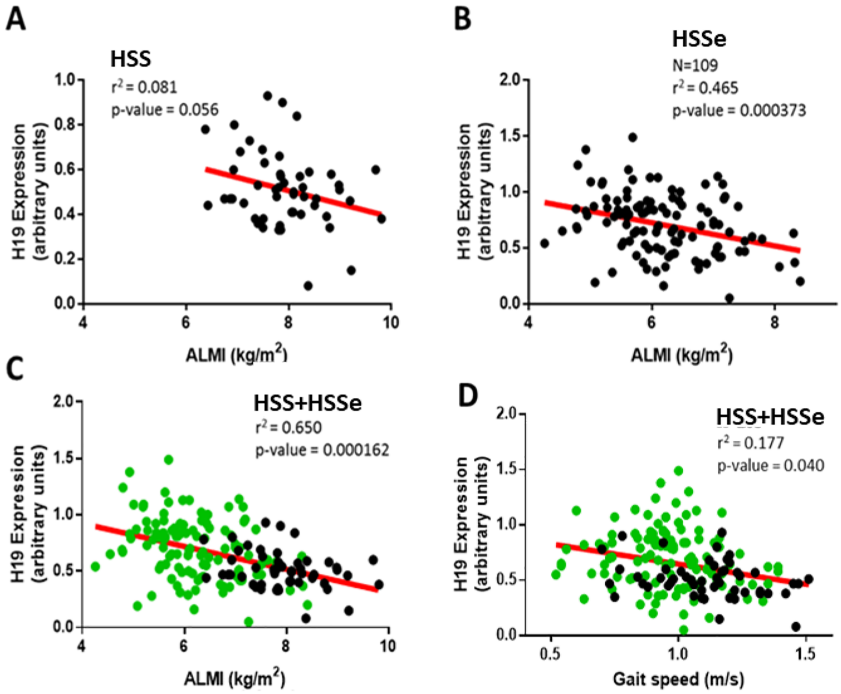

Table 3 Correlation between CpG methylation and H19 expression

CpG	Genomic coordinates (hg19)	*N*	Pearson *r*	*P*-value	95% CI (lower, upper)
CTCF6					
CpG-2098	Chr11:2021203+	77	−0.231	*0.043**	−0.430, −0.007
CpGs-2103/-2105	Chr11:2021208/10+	72	−0.245	*0.038**	−1.645, −0.049
CTCF3					
CpGs-4344/-4347/-4349/-4351	Chr11:2023449/52/54/56−	87	−0.211	*0.049**	−2.412, −0.002
CpGs-4288/-4290/-4294	Chr11:2023393/95/99−	87	−0.218	*0.042**	−2.599, −0.047

95% CI, 95% confidence interval.
*$P < 0.05$.

Table 4 Association between the methylation at CTCF sites and appendicular lean mass index

CpG	Genomic coordinates (hg19)	*N*	r^2	*P*-value	95% CI (lower, upper)
CTCF6					
CpG-2098	Chr11:2021203+	80	0.341	*0.036**	0.177, 4.965
CpGs-2103/-2105	Chr11:2021208/10+	74	0.373	*0.037**	0.141, 4.280
CTCF3					
CpGs-4344/-4347/-4349/-4351	Chr11:2023449/52/54/56−	93	0.307	0.831	−4.231, 3.327
CpGs-4288/-4290/-4294	Chr11:2023393/95/99−	93	0.299	0.506	−5.344, 2.656

95% CI, 95% confidence interval.
*$P < 0.05$.

Higher miR-675-3p/5p expression is associated with lower appendicular lean mass index

Exon 1 of *H19* encodes two conserved miRNAs, *miR-675-3p* and *miR-675-5p* (*Figure* 3A). We sought to investigate whether the expression of these miRNAs showed a similar association with ALMi, as observed with *H19*. We found in the combined HSS and HSSe data set that lower ALMi was associated with higher *miR-675-5p* (r^2 = 0.629, *P* = 0.005, *Figure* 3B) and *miR-675-3p* (r^2 = 0.598, *P* = 0.089, *Figure* 3C) expression. Both *mir-675-5p* and *mir-675-3p* showed a significant positive correlation with *H19* expression (*r* = 0.192, *P* = 0.017 and *r* = 0.182, *P* = 0.028, respectively) (*Figure* 3D and 3E and *Table S2*). There were however sex differences in the association between ALMi and *miR-675-3p* (men *P* = 0.074, women *P* = 0.42) and *miR-675-5p* (men *P* = 0.001, women *P* = 0.171).

miR-675-3p/5p expression is associated with altered SMAD1 and SMAD5 RNA and protein expression

SMAD1 and *SMAD5* mRNAs have been reported to be direct targets of *miR-675-3p*.[34] We found in the combined HSS and HSSe data set that higher *miR-675-3p* expression was associated with lower *SMAD1* and *SMAD5* mRNA expression (r^2 = 0.146, *P* = 0.003 and r^2 = 0.396, *P* = 0.034, respectively). *miR-675-5p* also showed an inverse association with *SMAD1* (r^2 = 0.140, *P* = 0.004) and *SMAD5* mRNA levels (r^2 = 0.391, *P* = 0.090, *Figure* 4A–4D and *Table S3*). Higher expression of both *miR-675-3p* and *miR-675-5p* was also associated with lower SMAD1 (r^2 = 0.792, *P* < 0.001 and r^2 = 0.760, *P* = 0.001, respectively) and SMAD5 (r^2 = 0.584, *P* = 0.011 and r^2 = 0.723, *P* = 0.001, respectively) protein levels

Figure 3 *miR-675-3p/5p* expression in skeletal muscle tissue. (*A*) Schematic of the *H19* gene, showing the localization of *miR-675* in exon 1 of the H19 gene. (*B*) Association between *miR-675-5p* expression and ALMi. (*C*) Association between *miR-675-3p* expression and ALMi. (*D* + *E*) Correlation between the expression of *miR-675-5p* (*D*) and *miR-675-3p* (*E*) with *H19*. Statistics are from multivariate regression models with adjustment for age and sex (*A* + *B*) and Pearson correlation analysis (*D* + *E*). Melt curves for *B* + *C* are in *Figure S2*.

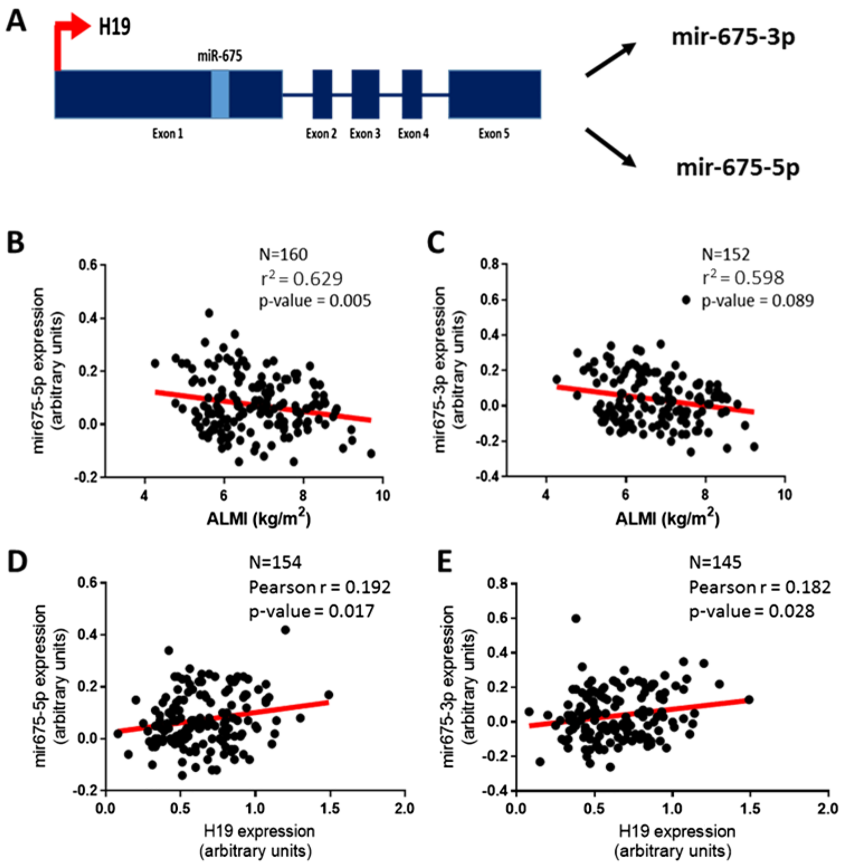

Figure 4 *SMAD1/5* RNA and protein expression in skeletal muscle and association with miR-675-3p/5p expression. (*A* + *B*) Association between *SMAD1* mRNA levels and *miR*-675-*3p* (*A*) and *miR-675-5p* (*B*) expression. (*C* + *D*) Association between *SMAD5* mRNA and *miR-675-3p* (*C*) and *miR-675-5p* (*D*) expression. (*E*) Representative western blot for SMAD1 and SMAD5 protein in skeletal muscle tissue, with β-actin as a loading control. Full blots are available in *Figure S5*. (*F–I*) Association between SMAD1 (*F* + *G*) and SMAD5 (*H* + *I*) protein levels and miR-675-3p (*F* + *H*) and miR-675-5p (*G* + *I*) expression. Statistics are from multivariate regression models with adjustment for age and sex (*Table S3*). Melt curve for *SMAD1/5* qRT-PCR are in *Figure S2*.

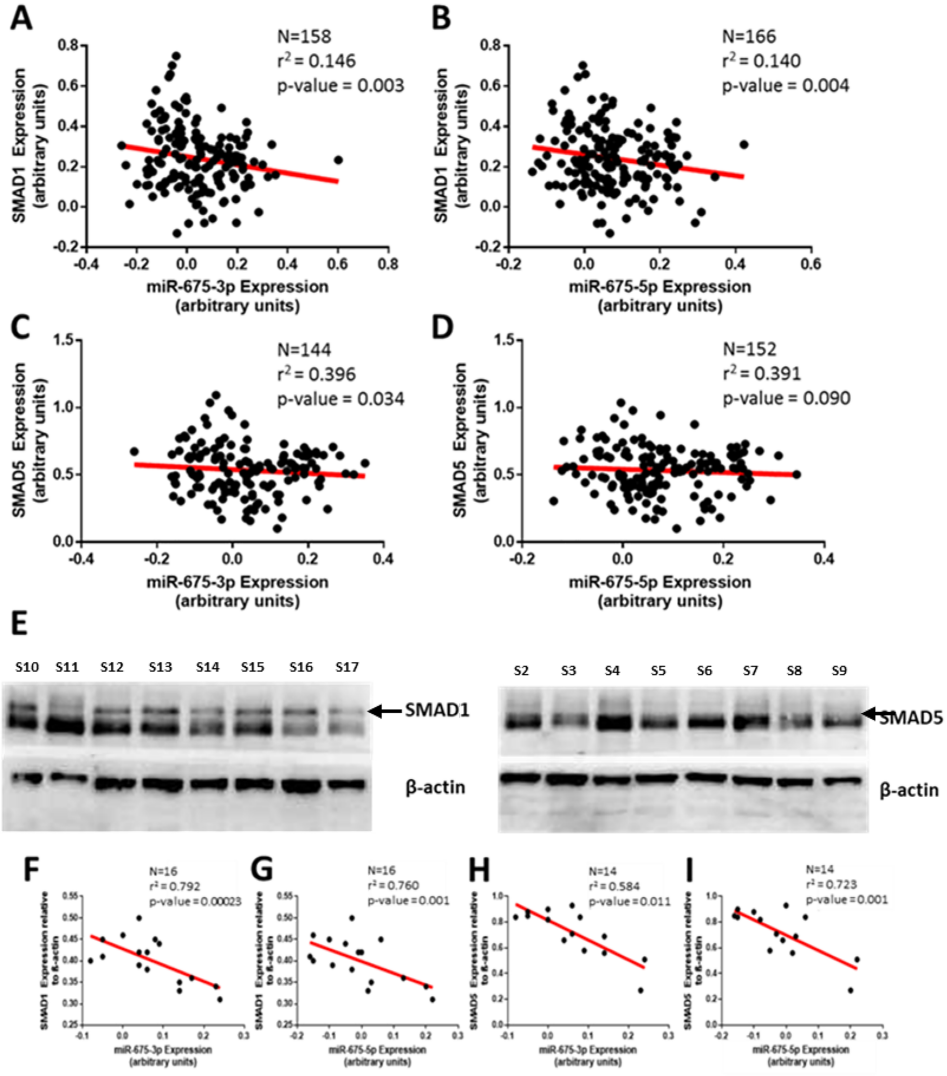

(*Figure* 4E–4I). Moreover, SMAD1 protein levels showed a positive association with ALMi (P = 0.048, r^2 = 0.856), although no association was observed between SMAD5 protein levels and ALMi (P = 0.376) (*Table S3*).

SMAD1/5 expression was associated with a reduction in type II muscle fibre size

As *SMAD1/5* expression has been linked to hypertrophy, we also examined the relationship between *SMAD1* and *5* expression and fibre size in muscle biopsies from HSS. Lower *SMAD1* and *5* mRNA expression was associated with a reduction in larger type II (fast) muscle fibres (*Figure* 5, r^2 = 0.184, P = 0.037 and r^2 = 0.246, P = 0.032, respectively). There was no association between *SMAD1* or *5* RNA levels and type I (slow) muscle fibre area (*Table S3*).

The H19/miR-675-3p/5p axis directly affects the expression of SMAD1/5

To determine whether alterations in the *H19/miR-675-3p/5p* axis can directly affect *SMAD1/5* expression in human primary muscle cells, we used a siRNA directed against *H19* to knock down the expression of *H19* in myotubes, differentiated from

DOI: 10.1002/rco2.44

Figure 5 Role of *H19-miR-675-SMAD1/5* axis in skeletal muscle hypertrophy. (*A*) A serial cross section showing differential fibre staining. Darkly stained fibres represent type II fast fibres. Bar represents 200 μM. (*B*) Association between *SMAD1* RNA expression and type II (fast) fibre area (μm^2). (*C*) Association between *SMAD5* RNA expression and type II (fast) fibre area (μm^2).

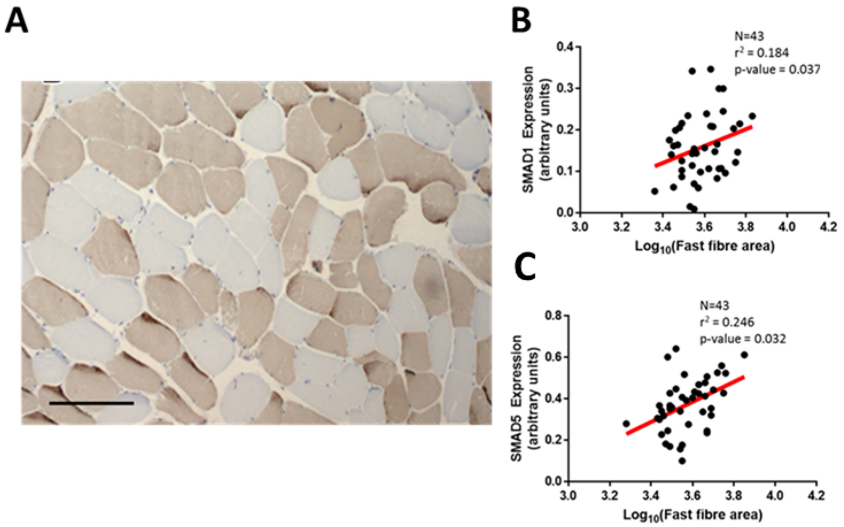

human primary myoblasts isolated from the HSSe muscle biopsies. Transfection of a siRNA against *H19* significantly decreased *H19* mRNA expression ($P = 0.005$), with a corresponding decrease in the expression of both *miR-675-3p* ($P = 0.009$) and *miR-675-5p* ($P = 0.050$) (*Figure* 6A). *H19* knockdown also induced a significant increase in levels of *SMAD1* and *SMAD5* mRNA ($P = 0.002$ and $P = 0.006$, respectively). To test whether *H19* acts through *miR-675-3p/5p*, to directly affect the expression of *SMAD1/5*, we introduced *miR-675-3p* and *miR-675-5p* mimics into the myotubes and found a significant decrease in *SMAD1* and *SMAD5* mRNA ($P = 0.030$ and $P = 0.020$, respectively) levels (*Figure* 6B), suggesting direct targeting of *SMAD1/5* by *miR-675-3p/5p*. Consistent with this, rescuing *miR-675-3p/5p* expression by ectopic expression of the miRNAs following *H19* siRNA knockdown also showed a decrease in *SMAD1* and *SMAD5* mRNA ($P = 0.008$ and $P = 0.032$, respectively) (*Figure* 6C).

Discussion

In this study, we report novel changes in the muscle transcriptome associated with low muscle mass in older individuals. We show that lower ALMi is associated with higher expression of the long non-coding RNA *H19* and its miRNA effectors *miR-675-3p* and *miR-675-5p*, and lower expression of the anti-differentiation SMAD transcription factors, *SMAD1* and *SMAD5*, which are direct targets of the microRNA, *miR-675-3p*. There was an inverse correlation between *H19* expression and DNA methylation within the H19 ICR, suggesting that epigenetic processes may initiate or maintain the differences observed in *H19* expression associated with changes in ALMi. Furthermore, we show that lower *SMAD1* and *5* mRNA expression was associated with a reduction in larger type II (fast) muscle fibres, suggesting that dysregulation of the *H19*/*miR-675*/SMAD pathway may block the anabolic signals associated with *SMAD1/5* expression, contributing and/or marking the loss of muscle mass in old age.

Regulation of muscle mass requires the interplay of multiple different genes and pathways.[35] The top transcript up-regulated in muscle tissue from individuals with high ALMi was SBK2, a serine/threonine-protein kinase, while the top transcript down-regulated in muscle samples from individuals with high ALMi was *H19*, a long non-coding RNA of 2.4 kb in length. Lewis *et al*. have previously reported that *H19* was up-regulated in COPD patients with low fat-free mass index (FFMi) and low muscle strength.[33] Our data would also suggest that higher *H19* expression is associated with loss of muscle mass in old age and may have the potential to act as a biomarker of muscle mass in the general population, rather than being specifically related to muscle wasting in COPD patients.

H19 has been reported to be highly expressed in embryonic tissues but down-regulated after birth in all tissues except skeletal muscle,[36] where it plays a pivotal role in muscle differentiation. *H19* expression is up-regulated during the differentiation of mouse C2C12 cells, and during mouse and human primary skeletal muscle satellite cell differentiation.[34,37,38] Moreover, knockdown of *H19* expression in C2C12 cells or human skeletal muscle cells leads to a decrease of myogenesis with a significant reduction in the expression of myogenic markers such as myogenin and MHC.[34]

Figure 6 Effect of siRNA-mediated *H19* knockdown and *miR-675-3p/5p* ectopic expression on *SMAD1/5* levels in human primary myotubes. RNA expression levels of *H19*, *miR-675-3p*, *miR-675-5p*, *SMAD1*, and *SMAD5* RNA (left to right) are shown in primary myotube cells following treatment with a scrambled siRNA (-ve) and *H19* siRNA (*A*), *miR-675-3p/5p* mimics (*B*), and *H19* siRNA and *miR-675-3p/5p* mimics (rescue) (*C*). Data are shown as mean ± SEM. $^{**}P < 0.01$, $^{*}P < 0.05$. All statistical analysis was paired-samples *t*-test (two-tailed), $n = 9$ per group.

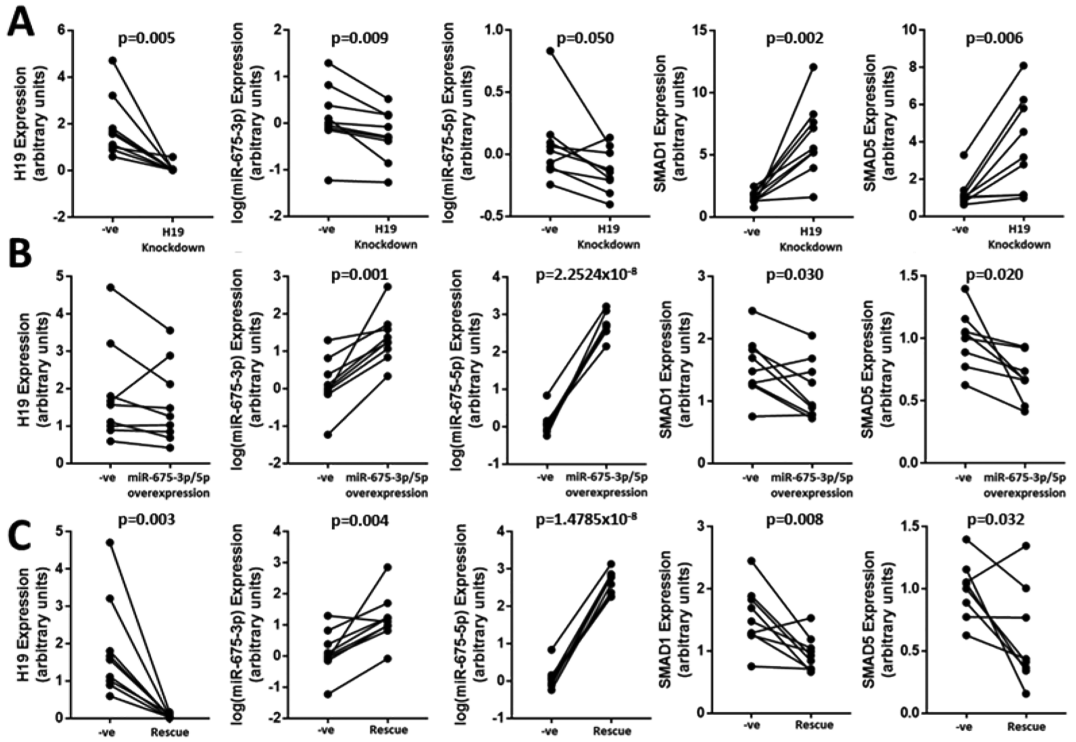

As H19 enhances muscle cell differentiation, the increase in *H19* expression observed in this study associated with low ALMi may indicate activation of regeneration and repair pathways in skeletal muscle from individuals with low muscle mass.[34]

Exon 1 of *H19* encodes two conserved microRNAs, *miR-675-3p* and *miR-675-5p*, and *H19* derived *miR-675* has been reported to play a major role in mediating the effects of *H19* on muscle cell differentiation. Dey *et al*.[34] showed that ectopic expression of either *miR-675-3p* or *miR-675-5p* rescued the reduction in muscle cell differentiation induced by *H19* knockdown in C2C12 cells and mouse and human satellite cells, suggesting that *miR-675-3p* and *miR-675-5p* are major contributors to the pro-differentiation function of H19. *miR-675-3p* and *miR-675-5p* may influence muscle differentiation by repressing the bone morphogenetic protein (BMP) pathway by targeting the SMAD transcription factors, SMAD1 and SMAD5, which are direct targets of *miR-675-3p*, and the cell division control protein 6 (*CDC6*), which is essential for the initiation of DNA replication, and a direct target of *miR-675-5p*. Interestingly co-knockdown of *SMAD1*, *SMAD5*, and *CDC6* in *H19* siRNA transfected C2C12 cells was sufficient to overcome the decrease in differentiation,[33] suggesting that these are important targets for the differentiation function of *H19*. We have shown that there was a positive association between *H19* expression and *miR-675-3p* and *miR-675-5p* expression in muscle biopsies and that higher expression levels of both *H19* and *miR-675-3p* and *miR-675-5p* were associated with lower muscle mass. In muscle tissue, there was also a negative association between *miR-675-3p* RNA expression with levels of *SMAD1* and 5 mRNA and protein levels, suggesting that dysregulation of H19/miR-675/SMAD1/5 pathway may be linked to loss of muscle mass in older individuals. Furthermore, knockdown of *H19* in primary human myotubes resulted in increased *SMAD1/5* RNA levels, while rescuing *miR-675-3p/5p* expression by ectopic expression of the miRNAs following *H19* siRNA knockdown led to a decrease in *SMAD1* and *SMAD5* mRNA levels, consistent with *SMAD1* and *5* being direct targets of *miR-675-3p* and suggesting that miRNA regulation of SMAD1/5 expression may be an important regulatory mechanism in human muscle cells.

Studies in animal models have shown that SMAD1 and 5 positively regulate skeletal muscle mass by promoting muscle growth and preventing muscle wasting.[39,40] Over-expression of BMP7 or the BMP receptor ALK3 in

skeletal muscle in mice leads to increased SMAD1/5/8 phosphorylation, increased muscle hypertrophy, and increased muscle fibre size, muscle mass, and force. Consistent with this, here, we found that lower *SMAD1* and *5* mRNA levels were associated with smaller type II fast-twitch muscle fibres. Muscle ageing has been associated with a reduction in type II fibres type,[41,42] which has been suggested to result from denervation of type II muscle fibres with collateral re-innervation of type I muscle fibres.[42] These results suggest that SMAD1/5, first shown to be important for maintaining muscle mass in animal studies, may also play a role in the loss of muscle mass in humans in old age. Further studies however will be required to determine whether SMAD1/5 and/or the H19/miR-675 pathway play a causal role in the loss of muscle mass in old age.

The expression of *H19* has been shown to be regulated by imprinting, where the *H19* gene is expressed from the maternal allele and expression from the paternal allele is silenced by DNA methylation. The *H19* gene has an ICR upstream from its transcription start site.[43] CTCF binding sites in the ICR play key roles in the maintenance of allele-specific expression of the gene. Interestingly, decreased *H19* expression was associated with an increase in methylation at two key CTCF sites, CTCF6 and CTCF3. The CpGs within the CTCF 6, CpGs-2103/-2105 and CpG-2098, the CpGs most strongly associated with H19 expression, were also positively associated with ALMi, suggesting that epigenetic mechanisms may play a role in initiating and/or maintaining the change in *H19* expression associated with lower ALMi and contribute to the loss of muscle mass in older individuals.

H19 expression was not associated with grip strength, which EWGSOP2 has recently proposed to be the primary parameter of sarcopenia diagnosis in clinical practice, prior to assessing muscle mass[2] through imaging techniques. Interestingly, our discovery of a robust association of high *H19/mir-675* with low muscle mass suggests that these non-coding RNAs could be used as biomarkers as an alternative approach to assess muscle mass. Non-coding RNAs especially miRNAs have been showed to be present at significant levels in extracellular bodily fluids, including blood serum and plasma. Exosomes or microvesicle encapsulated miRNAs are released from many cell types, including muscle,[44–46] and are thought to play a key role in communication between cells. Interestingly, recent studies have showed that specific muscle miRNAs have been detected in serum associated with the progression of muscle wasting in myotonic dystrophy type 1.[47] Further work will be needed to determine whether *miR-675* is detectable in serum and associated with loss of muscle mass and has potential as a biomarker of muscle quantity.

There are a number of limitations to this study. Firstly, we carried out the RNAseq analysis on male participants only; however, we did replicate the association observed between *H19* and ALMi using qRT-PCR in an independent group of both men and women from the HSSe cohort, suggesting that the association between the *H19* and ALMi is observed in both sexes. Lewis *et al*. also reported that higher expression of *miR-675* and its host gene *H19* were associated with lower FFMi in COPD patients although they found no association between *miR-675* expression and FFMi in a subset of muscle samples from participants from the HSS.[33] However, there were a number of differences between these studies. Here, we examined the relationship between *miR-675-3p* and *miR-675-5p* with ALMi, rather than FFMi. We also examined the expression of the two miRNAs generated from *H19*, *miR-675-3p*, and *miR-675-5p* in independent assays, rather than using a combined assay, and we were able to assess expression in a larger number of participants. Moreover, we observed associations between *H19*, its effector miRNAs, and the mRNA targets of *miR-675*, supporting the robustness of our current findings and suggesting that this axis is altered with respect to low muscle mass index. The second limitation to this study was that there was a relatively high number of participants who were overweight or obese in both the HSS and HSSe cohorts. However, adjusting for total body fat or % fat mass did not alter the list of transcripts significantly associated with ALMi. Thirdly, although we found changes in DNA methylation across CTCF sites within the H19 ICR associated with both *H19* expression and low muscle mass, the changes observed in DNA methylation were small. DNA methylation within a cell is binary; thus, the small differences in DNA methylation observed in the muscle samples are likely to represent changes in the number of cells expressing *H19* and/or differences in the cellular composition of the tissue with respect to ALMi, both of which may ultimately affect muscle function. Fourthly, because of the invasive nature of human muscle biopsies in volunteer participants, we only had low quantities of protein remaining for western blot analysis and further replication of the western blot analysis to assess SMAD protein expression is required. However, we did see a down-regulation of *SMAD1/5* mRNA expression in relation to *miR-675* expression, suggesting that *miR-675* may regulate *SMAD1/5* mRNA levels. Finally, we were only able to assess the effect of *H19* knockdown in primary human myotube cultures on *SMAD1/5* mRNA levels rather than at the protein level due to insufficient material. miRNAs repress gene expression by binding to their target mRNAs and either induce mRNA degradation or inhibit the translation of the mRNA. Here, we observed an increase in *SMAD1/5* mRNA levels upon H19 knockdown, which was reversed by the addition of miR-675 mimics, but whether SMAD1/5 translation was also affected requires further investigation. However, these experiments do suggest that *H19/miR-675/SMAD1/5* axis identified by Dey *et al*. in mouse C2C12 cells also operates in human myoblasts and may play a role in loss of muscle mass in older individuals.[34]

Conclusions

This study is the first to show that changes in *H19* expression in human skeletal muscle are associated with skeletal muscle mass in older people. Moreover, the increase in *H19* expression associated with low ALMi was accompanied by an increase in *miR-675-3p/5p* expression and a decrease in *SMAD1/5* mRNA, targets of *miR-675-3p*, suggesting that dysregulation of this pathway in individuals with lower ALMi may mark the activation of muscle repair/regeneration pathways and/or block anabolic signals associated with *SMAD1/5* expression. The finding that the *H19/miR-675/SMAD1/5* pathway may play a role in the loss of muscle mass in older individuals may allow the development of new intervention strategies to slow the age-related loss of muscle mass in later life using antagomirs,[48] designed to repress the miRNAs implicated in this pathway.

Funding

This work was carried out as part of the MEMOSA collaborative project involving the Nestlé Institute of Health Sciences (NIHS) and the EpiGen Consortium: an international alliance of researchers at Auckland UniServices Limited, New Zealand; University of Southampton, Centre for Biological Sciences; Medical Research Council Lifecourse Epidemiology Unit, University of Southampton, UK; Singapore Institute for Clinical Sciences of the Agency for Science, Technology and Research (A*STAR); National University of Singapore; and UWI Solutions for Developing Countries, University of the West Indies. This work was supported by grants from the Medical Research Council (MC_U47585827, MC_ST_U2055), Arthritis Research UK, National Osteoporosis Society, International Osteoporosis Foundation, Cohen Trust, NIHR Southampton Biomedical Research Centre, University of Southampton and University Hospital Southampton NHS Foundation Trust, and NIHR Musculoskeletal Biomedical Research Unit, University of Oxford. K.M.G. is supported by the UK Medical Research Council (MC_UU_20/4), the US National Institute on Aging of the National Institutes of Health under Award Number U24AG047867, the UK Economic and Social Research Council (ESRC), the Biotechnology and Biological Sciences Research Council (BBSRC) under Award Number ES/M0099X, the National Institute for Health Research [as an NIHR Senior Investigator (NF-SI-055-0042) and through the NIHR Southampton Biomedical Research Centre], the European Union's Erasmus+ Capacity-Building ENeASEA Project, and Seventh Framework Programme (FP7/2007-203). H.P.P. is supported by the National Institute for Health Research through the NIHR Southampton Biomedical Research Centre. This report is independent research, and the views expressed in this publication are those of the authors and not necessarily those of the National Health Service, the NIHR, or the Department of Health. The funding bodies had no role in any of the design, collection and analysis, interpretation of data, writing of the manuscript, or decision to submit for publication.

Author contributions

H.P.P. and A.A.S. set up and conducted the HSS. H.P.P. performed the fieldwork and muscle biopsies for HSS. A.A.S., H.C.R., C.C., and H.P.P. set up the HSSe study. R.D., S.S., A.M.B., and H.P.P. coordinated and conducted the fieldwork for HSSe. J.N.F., K.L., N.K., E.M., K.G., H.P.P., C.M., and A.S. designed and interpreted the transcriptomic study. E.A. and E.G. performed the laboratory analysis of the myoblast cultures. E.A., E.M., E.G., S.B., P.T., L.W., and A.C. provided statistical support. E.A. and K.L. wrote the first draft. All authors provided scientific input into the data analysis, and read and approved the final version of this manuscript.

Acknowledgements

We would like to thank the study participants as well as the HSS research nurses who greatly contributed to the success of the study: Norma Diaper, Sanchia Triggs, Andrea Staniford, and Gemma Rood. We thank Aline Charpagne and Patrick Descombes for help with genomics experiments. The authors of this manuscript certify that they comply with the ethical guidelines for authorship and publishing in the *Journal of Cachexia, Sarcopenia and Muscle*.[49]

Online supplementary material

Additional supporting information may be found online in the Supporting Information section at the end of the article.

Table S1. List of primers.
Table S2. Modelling of H19 and miR-675-3p/5p expression according to clinical parameters.
Table S3. Modelling of SMAD1/5 and miR-675-3p/5p expression.
Figure S1. Schematic of the different samples used from the Hertfordshire Cohort Study. Hertfordshire Sarcopenia Study (HSS) consisted of 105 males, of which 40 were randomly selected for RNAseq analysis. 34 of these samples had sufficient RNA for qRT-PCR analysis, with a further 18 samples from HSS included to increase sample size and power. The Hertfordshire Sarcopenia Study extension (HSSe) is an independent cohort consisting of 168 males and females, for which 38 males and 92 females had sufficient RNA for qRT-PCR. The data was combined (HSS + HSSe) to improve overall power.

To investigate the role of H19, 9 samples from HSSe (selected to represent a range of H19 expression) were used for H19 knockdown and *miR-675-3p/5p* overexpression analysis.

Figure S2. Melt curves for HSS + HSSe qRT-PCR.

Figure S3. Specificity of anti-SMAD1 (ab33902) antibody. (A) SMAD1 staining in 2 myoblast samples and 2 positive controls (untreated HeLa cell lysates and UV-treated HeLa lysates). Two bands are present in the myoblast samples, but only the top band is present in the HeLa controls lysates. (B) SMAD1 staining in 2 myoblast samples and 4 muscle tissue samples, showing the two bands as seen in the first image. (C) SMAD1 staining in the presence of a SMAD1 peptide (ab66722). The presence of the peptide competes binding of the SMAD1 antibody to the top band, however the bottom band is still present in all samples. The top band is used for quantification of SMAD1 protein levels in all subsequent experiments.

Figure S4. Full western blots images from figure 4. Lanes are labelled with their respective sample ID numbers. Lanes with † indicate a lane failing western blot QC due to gel/filter issues.

Figure S5. Association of H19 in muscle biopsies from HSS which had both RNAseq and qRT-PCR data. Statistics are from a multivariate regression model with adjustment for age.

Conflict of interest

E.M. and J.N.F. are full-time employees of the Société des Produits Nestlé SA. K.M.G. and H.P.P. have received reimbursement for speaking at conferences sponsored by companies selling nutritional products and are part of an academic consortium that has received research funding from Abbott Nutrition, Nestec, and Danone. E.A., E.S.G., P.T., S.J.B., A.S., C.M., T.F., C.C., K.M.G., and K.A.L. are part of academic research programmes that have received research funding from Abbott Nutrition, Nestec, and Danone. The other authors confirm that they have no conflicts of interest.

References

1. Clynes MA, Edwards MH, Buehring B, Dennison EM, Binkley N, Cooper C. Definitions of sarcopenia: associations with previous falls and fracture in a population sample. *Calcif Tissue Int* 2015;**97**:445–452.
2. Cruz-Jentoft AJ, Bahat G, Bauer J, Boirie Y, Bruyere O, Cederholm T, et al. Sarcopenia: revised European consensus on definition and diagnosis. *Age Ageing* 2019;**48**:601.
3. McCarthy JJ, Esser KA. Anabolic and catabolic pathways regulating skeletal muscle mass. *Curr Opin Clin Nutr Metab Care* 2010;**13**:230–235.
4. Cuthbertson D, Smith K, Babraj J, Leese G, Waddell T, Atherton P, et al. Anabolic signaling deficits underlie amino acid resistance of wasting, aging muscle. *FASEB J* 2005;**19**:422–424.
5. Fry CS, Drummond MJ, Glynn EL, Dickinson JM, Gundermann DM, Timmerman KL, et al. Aging impairs contraction-induced human skeletal muscle mTORC1 signaling and protein synthesis. *Skelet Muscle* 2011;**1**:11.
6. Delbono O. Neural control of aging skeletal muscle. *Aging Cell* 2003;**2**:21–29.
7. Shea KL, Xiang W, LaPorta VS, Licht JD, Keller C, Basson MA, et al. Sprouty1 regulates reversible quiescence of a self-renewing adult muscle stem cell pool during regeneration. *Cell Stem Cell* 2010;**6**:117–129.
8. Bigot A, Duddy WJ, Ouandaogo ZG, Negroni E, Mariot V, Ghimbovschi S, et al. Age-associated methylation suppresses SPRY1, leading to a failure of re-quiescence and loss of the reserve stem cell pool in elderly muscle. *Cell Rep* 2015;**13**:1172–1182.
9. Hepple RT. Mitochondrial involvement and impact in aging skeletal muscle. *Front Aging Neurosci* 2014;**6**:211.
10. Short KR, Bigelow ML, Kahl J, Singh R, Coenen-Schimke J, Raghavakaimal S, et al. Decline in skeletal muscle mitochondrial function with aging in humans. *Proc Natl Acad Sci U S A* 2005;**102**:5618–5623.
11. Barton ER, Morris L, Musaro A, Rosenthal N, Sweeney HL. Muscle-specific expression of insulin-like growth factor I counters muscle decline in mdx mice. *J Cell Biol* 2002;**157**:137–148.
12. Chambon C, Duteil D, Vignaud A, Ferry A, Messaddeq N, Malivindi R, et al. Myocytic androgen receptor controls the strength but not the mass of limb muscles. *Proc Natl Acad Sci U S A* 2010;**107**:14327–14332.
13. Hardman SE, Hall DE, Cabrera AJ, Hancock CR, Thomson DM. The effects of age and muscle contraction on AMPK activity and heterotrimer composition. *Exp Gerontol* 2014;**55**:120–128.
14. Langley B, Thomas M, Bishop A, Sharma M, Gilmour S, Kambadur R. Myostatin inhibits myoblast differentiation by down-regulating MyoD expression. *J Biol Chem* 2002;**277**:49831–49840.
15. Conboy IM, Conboy MJ, Smythe GM, Rando TA. Notch-mediated restoration of regenerative potential to aged muscle. *Science* 2003;**302**:1575–1577.
16. Brack AS, Conboy MJ, Roy S, Lee M, Kuo CJ, Keller C, et al. Increased Wnt signaling during aging alters muscle stem cell fate and increases fibrosis. *Science* 2007;**317**:807–810.
17. Liao ZY, Chen JL, Xiao MH, Sun Y, Zhao YX, Pu D, et al. The effect of exercise, resveratrol or their combination on sarcopenia in aged rats via regulation of AMPK/Sirt1 pathway. *Exp Gerontol* 2017;**98**:177–183.
18. Alway SE, Martyn JK, Ouyang J, Chaudhrai A, Murlasits ZS. Id2 expression during apoptosis and satellite cell activation in unloaded and loaded quail skeletal muscles. *Am J Physiol Regul Integr Comp Physiol* 2003;**284**:R540–R549.
19. Zahn JM, Sonu R, Vogel H, Crane E, Mazan-Mamczarz K, Rabkin R, et al. Transcriptional profiling of aging in human muscle reveals a common aging signature. *PLoS Genet* 2006;**2**:e115.
20. de Magalhaes JP, Curado J, Church GM. Meta-analysis of age-related gene expression profiles identifies common signatures of aging. *Bioinformatics* 2009;**25**:875–881.
21. Migliavacca E, Tay SKH, Patel HP, Sonntag T, Civiletto G, McFarlane C, et al. Mitochondrial oxidative capacity and NAD^+ biosynthesis are reduced in human sarcopenia across ethnicities. *Nat Commun* 2019;**10**:5808.
22. Zillikens M, Demissie C, Hsu S, Yerges-Armstrong YH, Chou LM, Stolk WC, et al. Large meta-analysis of genome-wide association studies identifies five loci for lean body mass. *Nat Commun* 2017;**8**:80.
23. Matteini AM, Tanaka T, Karasik D, Atzmon G, Chou WC, Eicher JD, et al. GWAS analysis of handgrip and lower body strength in older adults in the CHARGE consortium. *Aging Cell* 2016;**15**:792–800.
24. Syddall HE, Aihie Sayer A, Dennison EM, Martin HJ, Barker DJ, Cooper C. Cohort profile: the Hertfordshire cohort study. *Int J Epidemiol* 2005;**34**:1234–1242.
25. Patel HP, Syddall HE, Martin HJ, Stewart CE, Cooper C, Sayer AA. Hertfordshire

sarcopenia study: design and methods. *BMC Geriatr* 2010;**10**:43.
26. Patel HP, Al-Shanti N, Davies LC, Barton SJ, Grounds MD, Tellam RL, et al. Lean mass, muscle strength and gene expression in community dwelling older men: findings from the Hertfordshire Sarcopenia Study (HSS). *Calcif Tissue Int* 2014;**95**:308–316.
27. Patel H, Syddall HE, Martin HJ, Cooper C, Stewart C, Sayer AA. The feasibility and acceptability of muscle biopsy in epidemiological studies: findings from the Hertfordshire Sarcopenia Study (HSS). *J Nutr Health Aging* 2011;**15**:10–15.
28. Trapnell C, Pachter L, Salzberg SL. TopHat: discovering splice junctions with RNA-Seq. *Bioinformatics* 2009;**25**:1105–1111.
29. Anders S, Pyl PT, Huber W. HTSeq—a Python framework to work with high-throughput sequencing data. *Bioinformatics* 2015;**31**:166–169.
30. Love MI, Huber W, Anders S. Moderated estimation of fold change and dispersion for RNA-seq data with DESeq2. *Genome Biol* 2014;**15**:550.
31. Cashman NR, Covault J, Wollman RL, Sanes JR. Neural cell adhesion molecule in normal, denervated, and myopathic human muscle. *Ann Neurol* 1987;**21**: 481–489.
32. Patel HP, White MC, Westbury L, Syddall HE, Stephens PJ, Clough GF, et al. Skeletal muscle morphology in sarcopenia defined using the EWGSOP criteria: findings from the Hertfordshire Sarcopenia Study (HSS). *BMC Geriatr* 2015;**15**:171.
33. Lewis A, Lee JY, Donaldson AV, Natanek SA, Vaidyanathan S, Man WD, et al. Increased expression of H19/miR-675 is associated with a low fat-free mass index in patients with COPD. *J Cachexia Sarcopenia Muscle* 2016;**7**:330–344.
34. Dey BK, Pfeifer K, Dutta A. The H19 long noncoding RNA gives rise to microRNAs miR-675-3p and miR-675-5p to promote skeletal muscle differentiation and regeneration. *Genes Dev* 2014;**28**:491–501.
35. Egerman MA, Glass DJ. Signaling pathways controlling skeletal muscle mass. *Crit Rev Biochem Mol Biol* 2014;**49**:59–68.
36. Gabory A, Jammes H, Dandolo L. The H19 locus: role of an imprinted non-coding RNA in growth and development. *Bioessays* 2010;**32**:473–480.
37. Milligan L, Antoine E, Bisbal C, Weber M, Brunel C, Forne T, et al. H19 gene expression is up-regulated exclusively by stabilization of the RNA during muscle cell differentiation. *Oncogene* 2000;**19**: 5810–5816.
38. Xu X, Ji S, Li W, Yi B, Li H, Zhang H, et al. LncRNA H19 promotes the differentiation of bovine skeletal muscle satellite cells by suppressing Sirt1/FoxO1. *Cell Mol Biol Lett* 2017;**22**:10.
39. Winbanks CE, Chen JL, Qian H, Liu Y, Bernardo BC, Beyer C, et al. The bone morphogenetic protein axis is a positive regulator of skeletal muscle mass. *J Cell Biol* 2013;**203**:345–357.
40. Sartori R, Sandri M. Bone and morphogenetic protein signalling and muscle mass. *Curr Opin Clin Nutr Metab Care* 2015;**18**:215–220.
41. Brunner F, Schmid A, Sheikhzadeh A, Nordin M, Yoon J, Frankel V. Effects of aging on Type II muscle fibers: a systematic review of the literature. *J Aging Phys Act* 2007;**15**:336–348.
42. Deschenes MR. Effects of aging on muscle fibre type and size. *Sports Med* 2004;**34**:809–824.
43. Szabo PE, Tang SH, Silva FJ, Tsark WM, Mann JR. Role of CTCF binding sites in the Igf2/H19 imprinting control region. *Mol Cell Biol* 2004;**24**:4791–4800.
44. Guescini M, Guidolin D, Vallorani L, Casadei L, Gioacchini AM, Tibollo P, et al. C2C12 myoblasts release micro-vesicles containing mtDNA and proteins involved in signal transduction. *Exp Cell Res* 2010;**316**:1977–1984.
45. Le Bihan MC, Bigot A, Jensen SS, Dennis JL, Rogowska-Wrzesinska A, Laine J, et al. In-depth analysis of the secretome identifies three major independent secretory pathways in differentiating human myoblasts. *J Proteomics* 2012;**77**:344–356.
46. Forterre A, Jalabert A, Chikh K, Pesenti S, Euthine V, Granjon A, et al. Myotube-derived exosomal miRNAs downregulate Sirtuin1 in myoblasts during muscle cell differentiation. *Cell Cycle* 2014;**13**:78–89.
47. Koutsoulidou A, Photiades M, Kyriakides TC, Georgiou K, Prokopi M, Kapnisis K, et al. Identification of exosomal muscle-specific miRNAs in serum of myotonic dystrophy patients relating to muscle disease progress. *Hum Mol Genet* 2017;**26**:3285–3302.
48. Krutzfeldt J, Rajewsky N, Braich R, Rajeev KG, Tuschl T, Manoharan M, et al. Silencing of microRNAs in vivo with 'antagomirs'. *Nature* 2005;**438**:685–689.
49. von Haehling S, Morley JE, Coats AJS, Anker SD. Ethical guidelines for publishing in the *Journal of Cachexia, Sarcopenia and Muscle*: update 2019. *J Cachexia Sarcopenia Muscle* 2019;**10**:1143–1145.